

INFRASOUND SIGNALS AS BASIS FOR EVENT DISCRIMINANTS

Rodney W. Whitaker

Los Alamos National Laboratory

Sponsored by National Nuclear Security Administration
Office of Nonproliferation Research and Development
Office of Defense Nuclear Nonproliferation

Contract No. DE-AC52-06NA25396

ABSTRACT

Herein we summarize the first several months' effort in this research project of calculating the near-field infrasound signals generated by ground motion sources such as underground tests and earthquakes. Our approach is a direct application of the Rayleigh integral to the ground motion acceleration as seen by an observer at altitude near the source. The numerical integration is straightforward; however, the specification of the acceleration time history may be more difficult. Results of such calculations can, with good ground motion models for underground tests and earthquakes, be used to look for differences in the near-field infrasound signals that would be the basis for discriminants. So far, the work has concentrated on getting basic codes in place and on modeling underground test signals, which will be the emphasis of this contribution. There are 34 events for which model ground motion parameters were derived, earlier by others, from the ground motion data. We now have access to the Nevada Test Site (NTS) ground motion database. This can help in improving ground motion models for underground tests. Another new development was the successful application of a two-dimensional time-domain finite-difference code to this problem. The code was run with a time dependent velocity boundary condition and to a problem time of 40 seconds showing the acoustic signal in the 12 km by 12 km domain. Results from this code can be used to benchmark other codes. Another planned use for this near-field modeling work is to provide realistic initial conditions for long-range acoustic propagation codes.

Report Documentation Page

Form Approved
OMB No. 0704-0188

Public reporting burden for the collection of information is estimated to average 1 hour per response, including the time for reviewing instructions, searching existing data sources, gathering and maintaining the data needed, and completing and reviewing the collection of information. Send comments regarding this burden estimate or any other aspect of this collection of information, including suggestions for reducing this burden, to Washington Headquarters Services, Directorate for Information Operations and Reports, 1215 Jefferson Davis Highway, Suite 1204, Arlington VA 22202-4302. Respondents should be aware that notwithstanding any other provision of law, no person shall be subject to a penalty for failing to comply with a collection of information if it does not display a currently valid OMB control number.

1. REPORT DATE SEP 2007		2. REPORT TYPE		3. DATES COVERED 00-00-2007 to 00-00-2007	
4. TITLE AND SUBTITLE Infrasound Signals as Basis for Event Discriminants				5a. CONTRACT NUMBER	
				5b. GRANT NUMBER	
				5c. PROGRAM ELEMENT NUMBER	
6. AUTHOR(S)				5d. PROJECT NUMBER	
				5e. TASK NUMBER	
				5f. WORK UNIT NUMBER	
7. PERFORMING ORGANIZATION NAME(S) AND ADDRESS(ES) Los Alamos National Laboratory, PO Box 1663, Los Alamos, NM, 87545				8. PERFORMING ORGANIZATION REPORT NUMBER	
9. SPONSORING/MONITORING AGENCY NAME(S) AND ADDRESS(ES)				10. SPONSOR/MONITOR'S ACRONYM(S)	
				11. SPONSOR/MONITOR'S REPORT NUMBER(S)	
12. DISTRIBUTION/AVAILABILITY STATEMENT Approved for public release; distribution unlimited					
13. SUPPLEMENTARY NOTES Proceedings of the 29th Monitoring Research Review: Ground-Based Nuclear Explosion Monitoring Technologies, 25-27 Sep 2007, Denver, CO sponsored by the National Nuclear Security Administration (NNSA) and the Air Force Research Laboratory (AFRL)					
14. ABSTRACT see report					
15. SUBJECT TERMS					
16. SECURITY CLASSIFICATION OF:			17. LIMITATION OF ABSTRACT	18. NUMBER OF PAGES	19a. NAME OF RESPONSIBLE PERSON
a. REPORT	b. ABSTRACT	c. THIS PAGE			
unclassified	unclassified	unclassified	Same as Report (SAR)	9	

OBJECTIVES

Under the earlier Los Alamos National Laboratory (LANL) infrasound program measuring infrasound signals from underground nuclear tests (UGT) at the NTS, some work was done on finding discriminants between UGTs and earthquakes. Plots of wind-corrected infrasound pressure amplitude vs M_b and signal duration vs M_b showed promising separation of the two signal types. These results are shown in Figure 1 below. While the two groups were not perfectly separated in these variables, the results were encouraging in a search for possible discriminants. The result for duration is probably due to the longer duration of earthquake motion compared to the

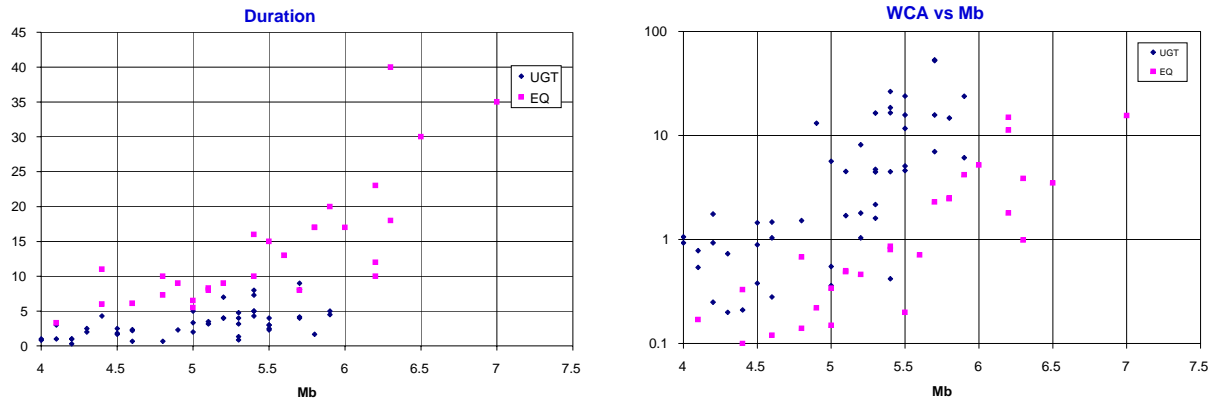


Figure 1. These figure illustrate the initial comparisons for UGTs and earthquakes for signal duration (left) and wind corrected amplitude (right) as functions of M_b .

relatively short duration for a UGT. On the other hand, UGT amplitudes would be larger due to the much larger ground motion at an UGT, although the larger area extent of the earthquake would be a competing factor.

The objective of this research is to find differences in the near-field infrasound signals of UGTs and earthquakes that can be the basis for establishing discriminants between the two sources. Such differences in the near-field would likely survive to longer range. Mutschlechner and Whitaker (2005) present an analysis of infrasound signals from earthquakes.

In this contribution we summarize a numerical technique to calculate the near-field infrasound signals generated by ground motion sources such as underground tests and earthquakes. Here we use a direct application of the Rayleigh integral to the ground motion acceleration as seen by an observer at an altitude near the source. The numerical integration is straightforward; however, the specification of the acceleration time history may be more difficult. For this contribution we emphasize results for UGTs.

RESEARCH ACCOMPLISHED

Background

In the early 1980s, LANL, under Department of Energy (DOE) funding, started a program to measure the ground motion induced acoustic signals from UGTs at the NTS. At the time, DOE was interested in technologies that could supplement seismic monitoring in the tasks of detection and yield estimation of UGTs. LANL infrasound arrays near St. George, UT, and at Los Alamos, NM, were in operation for almost every UGT from early 1983 until the end of US testing in September 1992.

Part of the LANL infrasound program included work on the propagation of infrasound signals to distances of 1000 km and sometimes farther. Because many of the NTS UGTs had some level of ground motion measurements in the form of acceleration records, it seemed that we could easily calculate the near-field infrasound signals from the UGTs. In addition, Sandia National Laboratories (SNL) fielded air-dropped pressure sensors over several tests (Banister et al., 1987) and had already started such calculations as a component of their program, Banister (1979). Around the same time, Lee and Walker (1980) developed another simple model for the parameterization of acceleration records from NTS tests, which highlighted some of the important parameters.

Rayleigh Integral

One can use the Rayleigh integral, Pierce (1989), to calculate the near-field pressure signal from a ground motion source with a specified acceleration history. The Rayleigh integral can be expressed as

$$p(R_0, t) = \frac{\rho}{2\pi} \int \frac{a(r, (t - R/c))}{R} dA_s \quad (1)$$

where a is the acceleration of the ground, r is a location on the ground (referenced to a center position), dA_s is an element of area on the ground, R is the distance from the ground element to the observing point, t is time, ρ is the air density, c is the speed of sound in air, p is the air pressure, and R_0 is the observation location. The Rayleigh integral geometry is shown in Figure 2, for a circular region of ground motion.

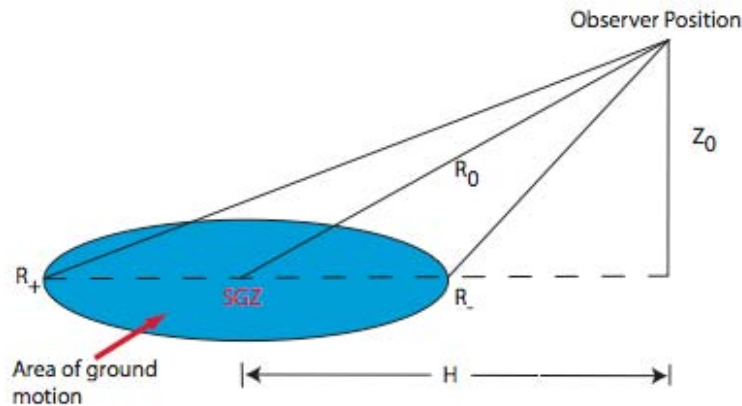


Figure 2: Illustration of the observer parameters in the Rayleigh integral technique. SGZ is the surface ground zero at the center of the ground motion, and R_+ and R_- indicate the extent of motion. The observer is at a horizontal distance H from SGZ and vertical distance Z_0 above SGZ, at a slant range of R_0 .

Real events can have departures from circular symmetry and this can be incorporated in the calculations. Specifying the acceleration as a function of position and time can be more difficult. A grid is set up on the ground dividing the area into a set of area elements as a function of range and angle from the center. The assumed acceleration model then gives the acceleration value as a function of time for each element.

Surface Ground Motion from UGTs

The surface ground motion from an UGT results from the propagation of the stress wave through the geology at the event to the surface. The simple model of ground motion acceleration from an UGT is that of a short impulse of acceleration, followed by deceleration to a minus one g phase due to spall (ballistic free fall) and concluding with the slap down impulse at spall closure. This is shown in Figure 3 (left figure). Spall is due to the reflection, at the free surface, of the upward elastic wave causing the ground to go into tensile failure and separate. The spall region free-falls briefly at $-1 g$, where g is the acceleration at the earth's surface. This model is quite oversimplified but is illustrative. The initial pulse can be complicated with plastic components. The slapdown pulse can show more detail as well. Small events may not enter into spall and therefore have no $-1 g$ phase. Even large events could be buried deep enough to minimize the surface ground motion; however, that would be expensive. At NTS the depth of burial (DOB) was selected based on containment criteria, the need to contain all radioactive gases in the ground and spall was often present in the records. A more complicated and real acceleration record from a Yucca Flats test at NTS,

taken from Jones et al. (1993), is shown in Figure 3 (right figure), which illustrates the additional features that may be present.

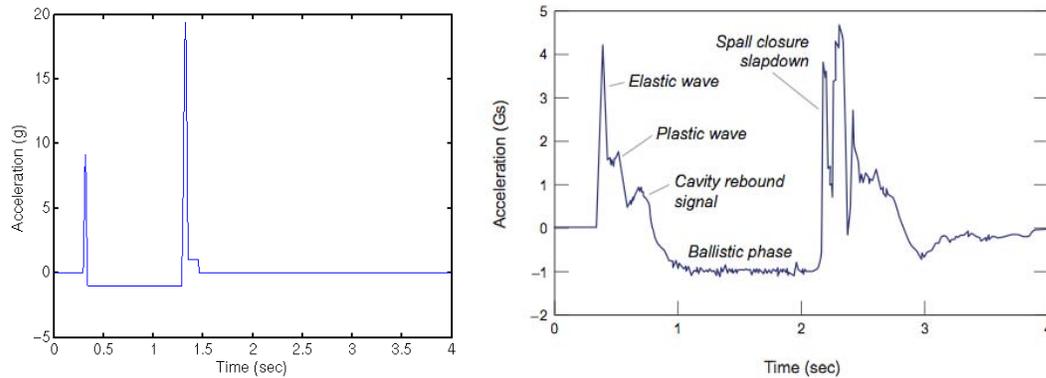


Figure 3: Simple model of ground motion from a UGT (left) showing acceleration (in g) vs time in seconds. A more complicated acceleration record is shown at the right.

In the case that the initial acceleration pulse is a short parabola with maximum acceleration A and width w , it is easy to show that the peak vertical velocity, V_{pk} is given by $2Aw/3$ at the end of positive acceleration and the vertical displacement at this time is given by $Aw^2/3$. As the velocity drops from the peak during the -1 g phase, the peak displacement occurs at the time when the velocity crosses zero and is

$$d_{pk} = \frac{Aw^2}{3} + \frac{V_{pk}^2}{2g} \quad (2)$$

The analysis in Lee and Walker (1980) leads to a number of insights based on a simple model of the ground motion acceleration. They point out that, after the initial acceleration pulse, the ground motion is determined by the peak velocity alone.

In the present work we are building off some earlier efforts using the Rayleigh integral method. That work followed the development given in Banister (1979) but used different accelerations models for UGTs. The numerical codes for the basic computations have been restored, and cases in the Banister report were reproduced, which served as a useful check. Also recovered were acceleration parameters for 34 NTS events, shown in Table 1 (see the end of this article), for which peak acceleration values and pulse widths for the elastic wave were determined along with the same for the plastic component and rebound signal, if they were present for the event. A simple exponential decay with range is assumed. These were determined from measured data for NTS UGTs in the NTS ground motion database, App and Tunnell (1994). However, detailed documentation on how these final parameters were determined has been lost. Nevertheless, Figure 4 shows two results for NTS events relating the wind corrected infrasound pressure amplitude (wca) to SGZ peak vertical velocity (left) and the wca as a function of near-field amplitude, Jones et al (1993).

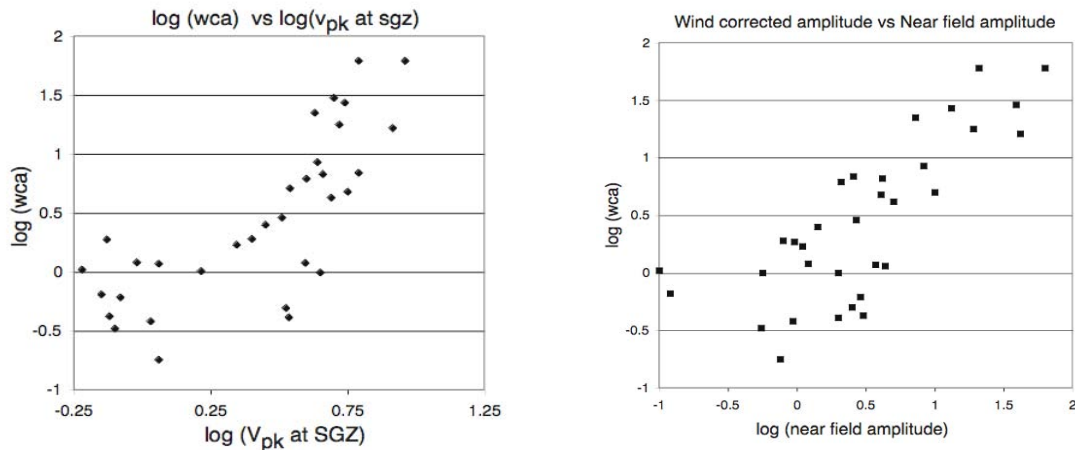


Figure 4: Wind corrected amplitudes (mbar) vs SGZ peak vertical velocity (m/s) on the left, and wind corrected amplitudes(mbar) vs computed near-field amplitudes (mbar). Wind corrected amplitudes are from the LANL, St. George, UT, infrasound array.

Other Ground Motion Models

In the current work we are working with surface accelerations, whether modeled or specified by actual measurements. Stump (1985) developed a momentum-conserving, equivalent body force model and included it in a normal moment tensor for use in synthetic seismograms. This reference summarizes much of the earlier work. Denny and Johnson (1991) review models for the seismic explosion source with comparisons to some data. Patton (1990) and Stump and Weaver (1992) examine data from NTS events on Pahute Mesa and examine relations for peak velocity and range decay behavior, among others.

Some Current Results

In Figure 6 we show some results of the current Rayleigh integral code for one of the 34 events with the modeled ground motion parameters. This case is for Towanda, U19ab, with a depth of burial of 660 m and the assumed elastic wave velocity was 2044 m/s, which determines the arrival time at a given slant range. One elastic arrival is assumed in this case. After slakedown, there is a damped oscillatory boundary condition applied to bring the final velocity to zero. Figure 5 shows the modeled acceleration record at SGZ for this event. For the pressure integration,

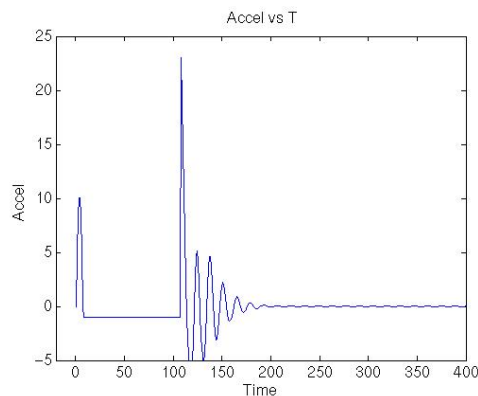


Figure 5: Modeled SGZ acceleration for U19ab, where accelerations are in g and time is in seconds.

the observer is at an altitude of 10km and the horizontal distances are 0 km, 1 km, 2 km, and then 3 km, and the results are shown in Figure 6. At 0 km range the looks similar to the velocity at SGZ exhibiting the on axis result for a uniform piston. In this case, the Rayleigh integral can be transformed, Pierce (1989), Lee and Walker (1980), so that the pressure is proportional to the difference in velocities at retarded times for the piston center and the retarded time at the piston edge. At the largest range, the large negative feature is due to nearly coherent arrivals from the spill region.

For reference purposes we show in Figure 7 the locations of the 34 events on a map of NTS with the areas outlined in yellow.

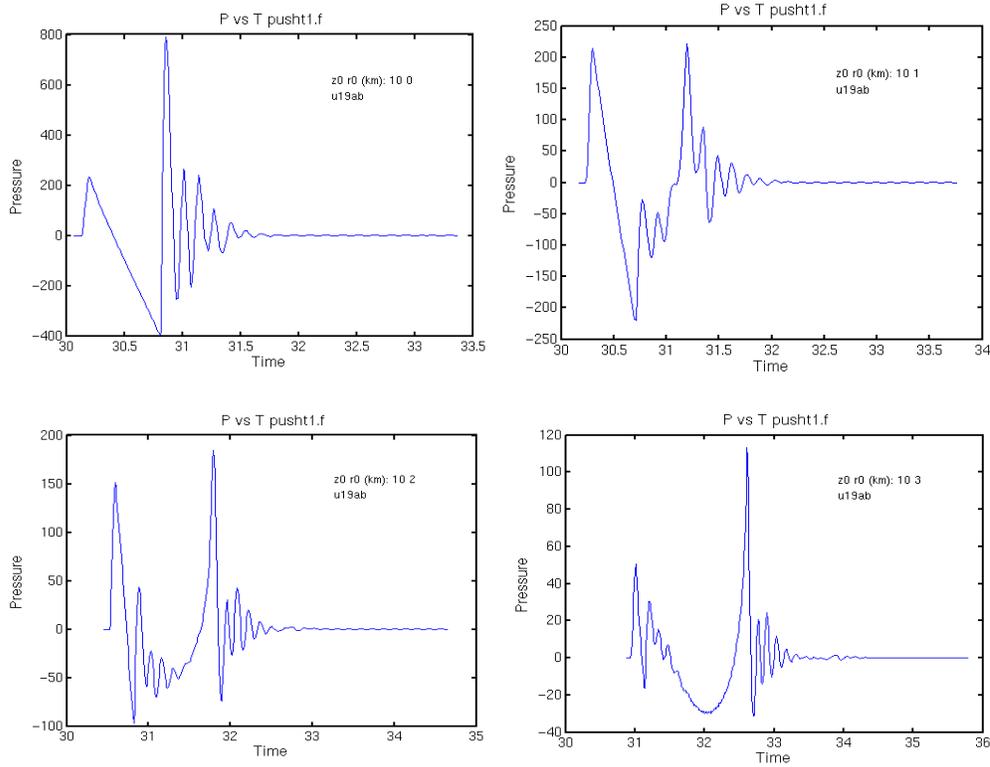


Figure 6: Near-field infrasound signals for ground motion modeled on U19ab. Pressures are in mbar and time in seconds. The observer altitude is 10 km and observer ranges are 0 km, upper left; 1 km, upper right; 2 km, lower left; and 3 km, lower right.

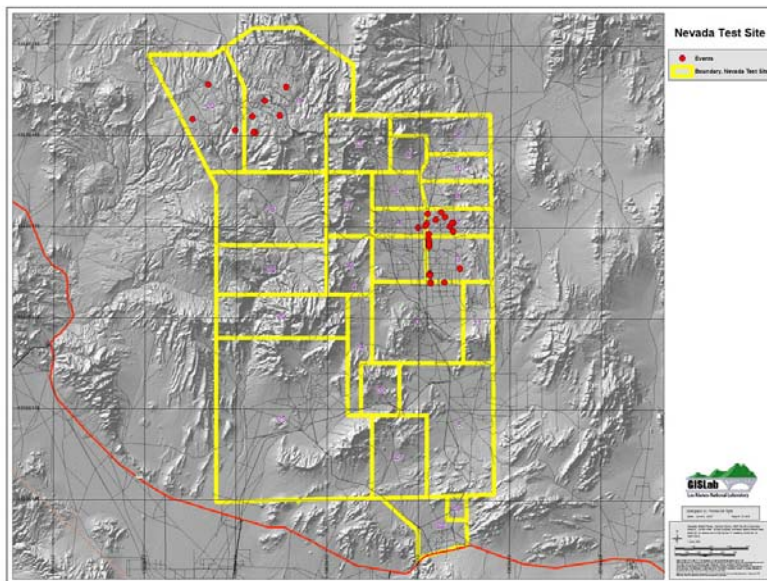


Figure 7: NTS map showing the locations of 34 events.

Two Unexpected but Useful Developments

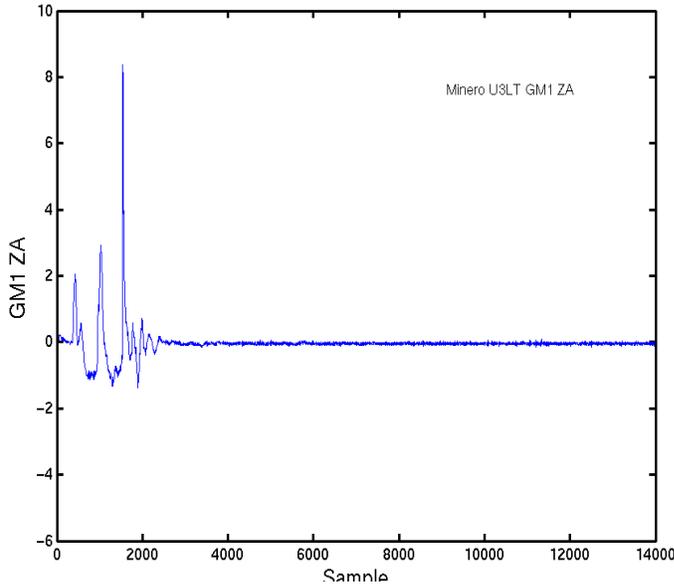


Figure 8: The SGZ acceleration record for the Minero event showing vertical acceleration vs sample number from the raw data file. Accelerations are in m/s^2 .

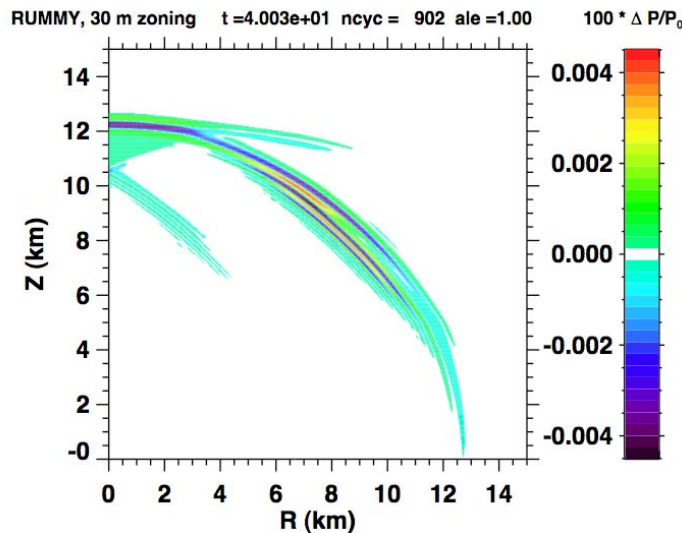


Figure 9: An acoustic signal as calculated by the CAVEAT code.

During this work, we obtained access to the data that had resided in the NTS ground motion database. This was the body of recorded ground motion data of accelerations and velocities for NTS UGTs. These seismic analysis code (SAC) files were provided by Allen Cogbill. Some events were well instrumented while others had a small number of stations. An example is shown in Figure 8, at left, for the Minero event at SGZ. These are raw data and some records contain noise spikes or other glitches that would need to be corrected before they could be directly used. Even so, they may provide verification of the Perak model parameters for the 34 events in Table 1. For events with sufficient ground motion stations, these could be used directly in the pressure integration.

Another unplanned development was a test application of the time-domain finite-difference numerical hydrodynamic code, CAVEAT (Addessio et al., 1992), to the calculation of the near-field infrasound signal from a ground motion source. In this two-dimensional, cylindrically symmetric (r, z) calculation, the mesh extends to just over 14 km in range and height. CAVEAT is used by the weapons phenomenology team at LANL and is a general computational fluid dynamics (CFD) program. For this test case, a time dependent velocity boundary condition was used at the surface and was somewhat based on ground motion data from event Rummy. Figure 9 shows contours of the pressure wave, $\Delta P/P_0$, in the calculation domain at 40 seconds. Variations of the signal with polar angle are easily seen. These calculations take longer than the Rayleigh integral but give results over the full domain. Inter-comparison of results from the two approaches may provide insight into the signal generation process.

CONCLUSIONS AND RECOMMENDATIONS

We have reviewed our recent work on calculating near-field infrasound signals from ground motion sources using acceleration records or parameterized modes. Our goal remains to look for discriminants between UGTs and earthquakes in the near-field as a basis for discriminants in the far-field signals observed by infrasound arrays. We summarized some results for work in the early 1990s related to the current work. The application of a time-domain, finite-difference fluid dynamics code will provide additional results for comparison.

While various runs are made for UGTs, we will begin to examine surface ground motion data and models for earthquake sources that can be incorporated into the current program. Characteristics of infrasound signals from a set of earthquakes are presented in Mutschlecner and Whitaker (2005), including some discussion of earthquake ground motions as they relate to the observed signals. Le Pichon et al. (2006) include an analysis of 12 earthquakes and plot their results for infrasound amplitude and duration vs M_S along with those in Mutschlecner and Whitaker (2005) with rather excellent agreement of the two data sets.

ACKNOWLEDGEMENTS

J. Paul Mutschlecner headed up the LANL infrasound effort during the period of underground testing and provided support and encouragement for many activities. This work benefited from and built upon earlier work by SNL researchers John Banister and Jack Reed and their co-workers. James J. Walker (LANL and later Amparo Corp) contributed to the analysis of UGT ground motion records. Eric Jones and Fred App used their knowledge of NTS UGT phenomenology to identify important characteristics of the surface ground motion as they related to test site area properties. Allen Cogbill provided a tar ball of SAC files of NTS ground motion measurements (acceleration, velocity and displacement) taken from the older ground motion database, App and Tunnell (1994). The CAVEAT calculation was performed by Eugene Symbalisky. Christy Flaming prepared two of the figures, and Thomas McTighe prepared the NTS map.

REFERENCES

- Addessio, Frank L., John R. Baumgardner, John K. Dukowicz, Norman L. Johnson, Bryan A. Kashiwa, Rick M. Rauenzahn, and Charles Zemach (1992). CAVEAT: A computer code for fluid dynamics problems with large distortion and internal slip, Los Alamos National Laboratory technical report, LA-10613-MS, Rev. 1.
- App, Frederick N. and Thomas Tunnell (1994). User manual for the NTS ground motion database retrieval program: ntsgm, Los Alamos National Laboratory technical report, LA-UR-94-1538.
- Banister, J. R. (1979). A program for predicting ground motion induced air pressures, Sandia National Laboratories report SAND 78-2361.
- Banister, John R., William V. Hereford, and Otis M. Solomon (1987). Preliminary results of MUNDO high altitude pressure measurements, Sandia National Laboratories report, SAND 86-2885.
- Denney, Marvin D. and Lane R Johnson (1991). The explosion seismic source function: Models and scaling laws reviewed. *Explosion Source Phenomenology*, Geophysical Monograph 65. Washington, DC: American Geophysical Union.
- Jones, Eric M., Frederick N. App, and Rodney W. Whitaker (1993). Ground motions and the infrasound signal: A new model and the discovery of a significant cavity rebound signal, Los Alamos National Laboratory technical report LA-UR-93-861.
- Lee, Huan and James J. Walker (1980). Model for ground motion and atmospheric overpressure due to underground nuclear explosions, Los Alamos Scientific Laboratory Report LA-8554-MS.
- Le Pichon, A., P. Mialle, J. Guilbert, and J. Vergoz (2006). Multistation infrasonic observations of the Chilean earthquake of 2005 June 13, *Geophys. J. Int.* 167: 838–844.
- Mutschlecner, J. Paul and Rodney W. Whitaker (2005). Infrasound from earthquakes, *J. Geophys. Res.* 110: D01108, doi:10.1029/2004JD0050067.

29th Monitoring Research Review: Ground-Based Nuclear Explosion Monitoring Technologies

- Patton, Howard J. (1990). Characterization of spall from observed strong ground motions on Pahute Mesa, *Bull. Seism. Soc. Am.* 80: 1326.
- Perret, William R. (1976). Surface motion Induced by nuclear explosions beneath Pahute Mesa, Parts I and II, Sandia National Laboratories report SLA-74-0348.
- Pierce, Allan D. (1989). *Acoustic: An Introduction to Its Physical Principles and Applications*. New York: Acoustical Society of America.
- Stump, Brian W. (1985). Constraints on explosive sources with spall from bear-source waveforms, *Bull. Seism. Soc. Am.* 75: 361.
- Stump, Brian W. and Thomas A. Weaver (1992). Physical models of spall zone ground motions and the determination of decay rates, Los Alamos National Laboratory technical report LA-UR-92-451.
- Wecksung, George W. (1985). Acoustic radiation patterns associated with the ground motion produced by a contained nuclear explosion, Amparo Corporation report (unpublished).

Table 1. Events with modeled ground motion parameters

Event Name	Hole	Longitude	Latitude	Date
ABILENE	U3MN	-116.04519	37.013115	4/7/88
ALAMO	U19AU	-116.377558	37.252395	7/7/88
AMARILLO	U19AY	-116.354441	37.275412	6/27/89
ATRISCO	U7BP	-116.007419	37.084155	8/5/82
BARNWELL	U20AZ	-116.410277	37.231037	12/8/89
BEXAR	U19BA	-116.313782	37.296033	4/4/91
CABRA	U20AJ	-116.460926	37.30063	3/26/83
CAPROCK	U4Q	-116.048917	37.103086	5/31/84
COALORA	U3LO	-116.04621	37.056108	2/11/83
DALHART	U4U	-116.050126	37.088955	10/31/88
DIVIDER	U3ML	-115.988778	37.020635	9/23/92
DOLCETTO	U7BI	-116.000232	37.089754	8/30/84
DUORO	U3LV	-116.043924	37.000333	6/20/84
GLENCOE	U4I	-116.066905	37.082962	3/22/86
HERMOSA	U7BS	-116.033208	37.094766	4/2/85
HOUSTON	U19AZ	-116.37212	37.22737	11/14/90
KINIBITO	U3ME	-116.046234	37.053224	12/5/85
LAREDO	U3MG	-116.043939	36.998551	5/21/88
LOCKNEY	U19AQ	-116.37559	37.227947	9/24/87
MINERO	U3LT	-116.04557	37.011903	12/20/84
MOGOLLON	U3LI	-116.046915	37.011614	4/20/86
MUNDO	U7BO	-116.023247	37.10618	5/1/84
PONIL	U7BV	-116.002632	37.089767	9/27/85
SALUT	U20AK	-116.489947	37.247799	6/12/85
TAHOKA	U3MF	-116.046171	37.060915	8/13/87
TAJO	U7BL	-116.016377	37.098248	6/5/86
TEXARKANA	U7CA	-116.001477	37.076741	2/10/89
TORNERO	U3LL	-116.045553	37.010645	2/11/87
TORTUGAS	U3GG	-116.04716	37.065727	3/1/84
TOWANDA	U19AB	-116.326088	37.253358	5/2/85
TURQUOISE	U7BU	-116.046822	37.072795	4/14/83
VAUGHN	U3LR	-116.046195	37.058031	3/15/85
VERMEJO	U4R	-116.053674	37.085186	10/2/84
VILLITA	U3LD	-116.018242	37.000059	11/10/84